Геология и геофизика, 2015, т. 56, № 12, с. 2263—2274

УДК 550(55), 553.7+550.831

ИССЛЕДОВАНИЕ КОНТРАСТОВ ПЛОТНОСТИ И ГЕОЛОГИЧЕСКИХ СТРУКТУР НА ГОРЯЧИХ ИСТОЧНИКАХ В ПРОВИНЦИИ МАРКАЗИ (ИРАН) С ИСПОЛЬЗОВАНИЕМ МЕТОДА ГРАВИТАЦИИ

Д. Нурали[1], С. Порхиал[2], М.М. Могхаддам[3], С. Мирзаели[4], Д. Эбрахими[5], М.Р. Рахмани[6]

[1] *Research Assistant Professor, Niroo Research Institute (NRI), Tehran, Iran*

[2] *Assistant Professor, Islamic Azad University, Karaj Branch, Iran*

[3] *PhD Student of Geophysics, Research Institute of Applied Sciences, Tehran, Iran*

[4] *Associate Professor, Research Institute of Applied Sciences, Tehran, Iran*

[5] *PhD Student of Geology, Niroo Research Institute, Tehran (NRI), Iran*

[6] *PhD Student of Geology, Renewable Energy Organization of Iran (SUNA), Tehran, Iran*

В 2012 году обновленная энергетическая организация Ирана (СУНА) провела исследование силы тяжести над горячим источником геотермального поля Махаллат в провинции Маркази (Центральный Иран) в рамках освоения региона и разработки программы исследования геотермальной энергии в нем. В регионе Махаллат находится самое большое геотермальное поле в Иране. В данной работе представлена интерпретация различных гравитационных карт и 3D инверсионной модели. На карте остаточной гравитации показаны три зоны отрицательной аномалии силы тяжести (A1, A2 и A3), связанные с региональными геотермальными источниками. Карты горизонтального градиента выявляют сложную систему разломов. Для того чтобы получить более подробную информацию о геотермальном источнике Хорхе, рассчитана 3D-модель контрастов плотности с использованием метода Ли-Ольденбурга. Полученная 3D-модель дает изображение глубинной эволюции и контрастов плотности и показывает, что зона A1 обладает высоким потенциалом для развития геотермальных источников. Результаты также показывают, что интервал глубин между 1000 и 3000 м в зоне A1 является наиболее эффективным для использования геотермальной энергии.

Сила тяжести, геотермальная система, аномалия Буге, Эйлер, инверсия, Махаллат

INVESTIGATION OF DENSITY CONTRASTS AND GEOLOGIC STRUCTURES OF HOT SPRINGS IN THE MARKAZI PROVINCE OF IRAN USING THE GRAVITY METHOD

J. Nouraliee, S. Porkhial , M. M. Moghaddam, S. Mirzaei, D. Ebrahimi, M. R. Rahmani

In 2012, the renewable energy organization of Iran (SUNA) performed a gravity survey around hot springs of the Mahallat geothermal field in the Markazi Province of Central Iran, as part of the explorations and developments of geothermal energy investigation program in the region. The Mahallat region has the greatest geothermal field in Iran. This work presents interpretation results of various gravity maps and a calculated 3D inversion model. The residual gravity map shows three negative gravity anomaly zones (A1, A2, and A3) associated with the geothermal reservoirs in the region. The horizontal gradient maps reveal a complex fault system. In order to attain more information about the Khorhe geothermal reservoir, a 3D density contrast model was calculated using the Li–Oldenburg method. The attained 3D model provides an in-depth image of the evolution, showing the density contrast and the A1 zone having a high potential for the geothermal reservoir in the region. The results also show that the rocks which exist between 1000 and 3000 meters under the Earth's surface in the Al zone are the most suitable aquifers for utilization of geothermal energy.

Gravity, geothermal system, Bouguer anomaly, Euler, inversion, Mahallat

INTRODUCTION

In geothermal exploration, gravity method generally is used to delineate subsurface structures that control the geothermal system. Basically, a given geothermal reservoir and its fluid content cause density differences between geothermal reservoir and the surrounding rocks. The basis of gravity method is density contrast in the rocks. Gravity studies in different regions of the world have yielded useful results for geothermal exploration, such as: investigation of topography of basement in a geothermal field (Salem et al. 2005; Soengkono, 2011),

✉e-mail: mmz140@yahoo.com

DOI: 10.15372/GiG20151211

magma chambers and intrusive body related to the heat source of the geothermal system (Represas et al., 2013) and delineation of faults and fractured zones corresponding to the reservoir of geothermal system (Abiye and Haile, 2008; Gottsmann et al., 2008; Montesinos et al., 2003; Represas et al., 2013; Salem et al., 2005; Schiavone and Lodo, 2007). Therefore, gravity method is one of the most economic geophysical methods for modeling of a geothermal system.

Mahallat geothermal field of Markazi province in Iran is a popular tourist destination due to the occurrence of hot springs and one of the richest geothermal fields in Iran. According to the available scientific data about Abgarm geothermal region, it is found that in the NW of Mahallat city has favorable conditions for the exploitation of geothermal energy. The local heat flow and the temperature maxima in the Mahallat geothermal field originate from strong convectional heat transport mainly in the igneous basement.

In the current study area, several studies have been conducted by the renewable energy organization of Iran (SUNA) and other research institutes. Using a ground magnetic study Oskooi at al. (accepted for publication) and Mirzaei et al. (2013) showed that heat source of the Mahallat geothermal system originates from a hot igneous intrusive mass which exists at the depth of more than 1.5 km at the east of Mahallat hot springs. Based on geological and geochemical studies, it was revealed that the hydrothermal fluids cycle in the area was controlled mainly by N–S faults (Porkhial et al., 2013). Using a Magnetotelluric (MT) survey along the 8 km-long profile over the Mahallat hot springs, Oskooi et al. (2013) and Oskooi and Darijani (2013) it is determined that Mahallat geothermal system included a cap rock (from 100 to 600 m), a reservoir (from 500 to 2000 m) and a source (from 1000 m to the deepest reachable point). However, these results can't illustrate the lateral extent of the structures of Mahallat geothermal system, because their interpretation was two-dimensional, and the amount of data was insufficient.

Gravity survey which is presented in this paper is the most important geophysical study conducted in Mahallat geothermal region that allows us to generate a comprehensive overview of the area. The only other performed geophysical and geological surveys are too local and incomplete to be of any use for this purpose. In the current study, a total of 380 gravity observations along several regular profiles were recorded, covering nearly 200 km^2.

It should be mentioned that so far no wells have been drilled in Mahallat geothermal region. Therefore all the data about this region are based on the surface studies.

GEOLOGICAL SETTING

In the Markazi province of Iran (Fig. 1), the geological structures are characterized by a dextral rotational movement, which has formed by northward under-thrusting of the Arabian plate beneath Central Iran (McKenzie, 1972). The Cenozoic geologic history and the stratigraphy of this region are complex, due to its tectonic framework. As a result, the stratigraphic record of the area is made up of units with different structural characteristics. During the Eocene, igneous activities took place in this area, causing accumulation of volcanic rocks over the Mesozoic and Paleozoic sediments. Subsequently, these rocks were thermally metamorphosed by an Early Miocene monzonitic batholith, elongated in a NW–SE direction.

Being the most important thermal water sources of the area, Abgarm hot springs are located 15 km northeast of Mahallat city in Markazi province. They are considered as a small part of the Central Iran zone, which is located in the Urumieh–Dokhtar volcanic belt. The geological setting of this area and the distribution of hot springs are presented in Fig. 1. The study area is characterized by sedimentary deposits from the Permian to the Quaternary, with the existence of magmatic and volcanic outcrops. Notable formations cropped out in the study area include the Shemshak Formation (shale and sandstone), Cretaceous Orbitolina bearing limestones, marly limestones of the Qom Formation and volcanic rocks (granodiorite, tuff and lava). The hot springs (depicted as orange hexagons in the geological map in Fig. 1) caused deposition of travertine sediments with considerable thickness of about 500 m. In this area, faults and fracture zones played an important role in the circulation of water from the surface down to the deep levels. Some important alterations have also been documented for the area.

Some major faults have been identified in the region. Generally, they have two main directions, NW–SE and NE–SW. The main geological feature present in the current study area is the segment of the NNE–SSW Mahallat–Abgarm fault (MAf) zone (Nouraliee and Shahhosseini, 2012). This structure stretches for 50 km, from southeast of Mahallat city to the north of Abgarm. All of the Abgarm hot springs is directly connected to this fault zone.

Geothermal surface manifestations

The area of the Abgarm region is composed of young volcanic rocks, hydrothermally altered zones, wide travertine outcrops and intrusive bodies as well. All of the hot springs are genetically related to tectonic activities and concentrated along the MAf zone. Due to the hot spring activity, a lot of travertine deposits have been

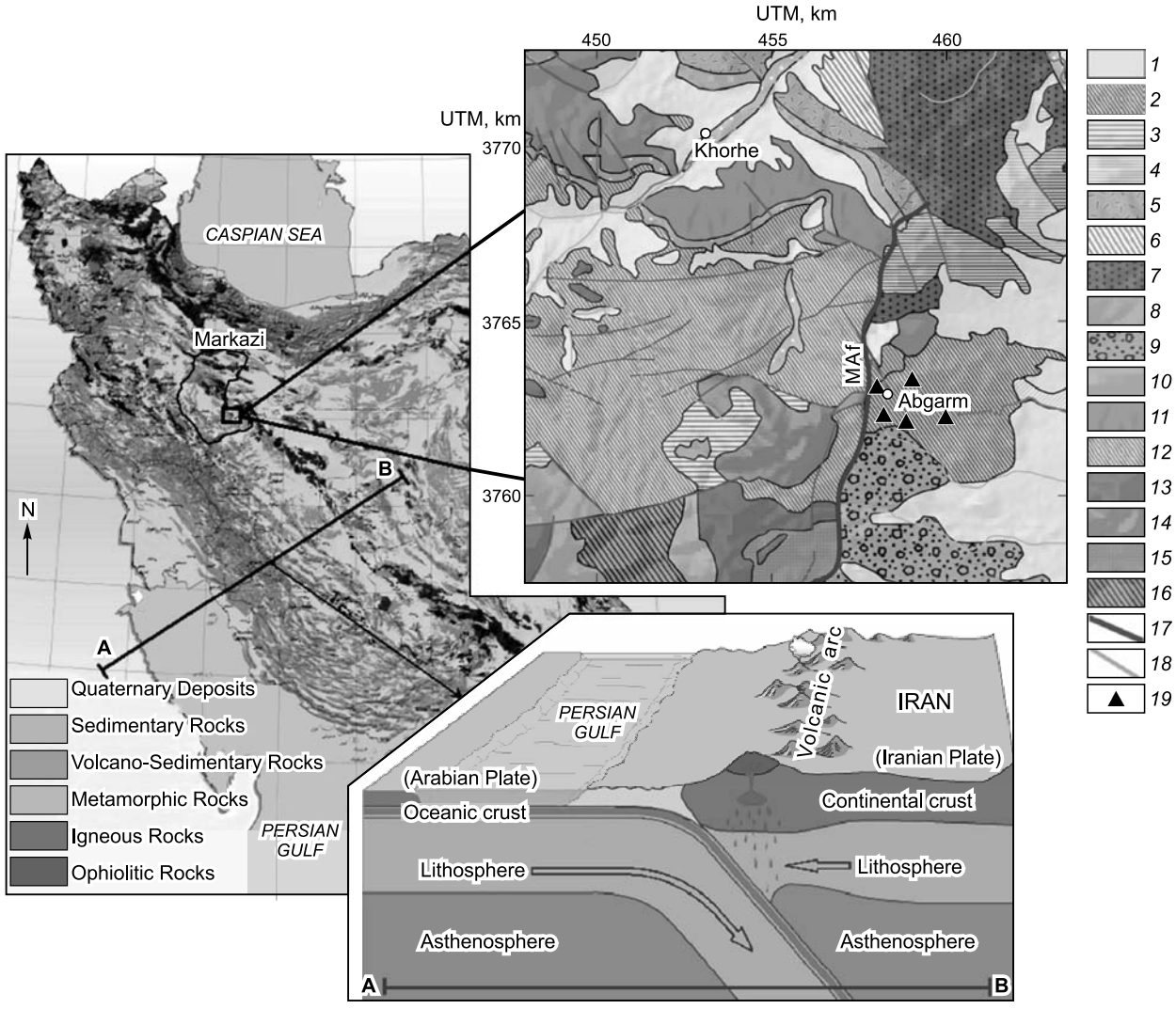

Fig. 1. Study area in the Markazi province of Iran, plate tectonic structure and large scale geological map adopted from 1:25,000 geological map published by NRI (Nouraliee and Shahhosseini, 2012).

Legend of geological map: ***1***, trace and fan (Quaternary); ***2***, travertine (Quaternary); ***3***, Limestone with fossile fragments (Tertiary); ***4***, marl (Oligocene); ***5***, ignimbrite and rhyolite (Eocene); ***6***, green tuff and tuffite (Eocene); ***7***, granite and granodiorite (Eocene); ***8***, conglomerate and sandstone (Eocene); ***9***, sandy conglomerate (Eocene); ***10***, sandstone and siltstone (Cretaceous); ***11***, limestone and sandstone (Jurassic); ***12***, shale and sandstone (Jurassic); ***13***, dolomitic limestone (Jurassic); ***14***, limestone and dolomite (Permian–Jurassic); 15, shale (Permian); ***16***, dolomite (Cambrian); ***17***, Main Mahallat–Abgarm fault (MAf); ***18***, fault; ***19***, hot spring.

accumulated in the Mahallat region. Travertine is a chemically-precipitated continental limestone formed around seepages, hot springs and along streams and rivers. It consists of calcite or aragonite, of low to moderate inter-crystalline porosity and often high mouldic or framework porosity within a vadose or occasionally shallow phreatic environment. Precipitation results primarily through transfer (evasion or invasion) of carbon dioxide from or to a groundwater source leading to calcium carbonate super-saturation, with nucleation/crystal growth occurring upon a submerged surface (Pentecost, 2005). Travertine deposits usually formed around hot springs can be a useful sign of geothermal activity in a region, either active or fossil one. Irregular fault movements can be responsible for spring migration leading to the deposition of a range of travertines at different levels (Soligo et al. 2002).

Before gravity studies, geological and geochemical studies were conducted in the area. In geological investigations, a very accurate 1:25,000 scale geological map of the Mahallat geothermal area was generated (Nouraliee and Shahhosseini, 2012). All faults and lithological units were studied in detail. Moreover, hydrothermally altered areas were recognized by Aster satellite images. They were also visited and sampled in order to perform mineralogical analysis.

Based on the Aster satellite images studies, checking outcrops and petrography studies, several altered zones were found in the study area. The most important of alteration types include argillitization-sericitization and kaolinitization-alunitization. Argillitization-sericitization alteration is detected in a close relationship with hydrothermal fluid activities. This type of alteration is representative of high-temperature geothermal systems. Previous studies suggest that the heat source of hot springs is due to the cooling processes of the molten magma (Oskooi et al., accepted for publication). Hot springs are charged by meteoric waters mixed with magmatic fluids (Beitollahi, 1996; Oskooi and Darijan, 2013). The hydrology and geothermometry studies (Rezaie et al., 2009) showed the average temperature of the hot springs to be about 46 °C and their pH to range from acidic to neutral. The water of hot springs is saturated by calcite minerals, hinting that the geothermal reservoir is probably formed in limestone.

A useful way for characterizing of various types of geothermal waters is to use chloride-sulphate-bicarbonate ternary diagram described by Giggenbach (1991). Based on the chemical data, it was found that the Mahallat hot springs are slightly acidic and sulphatic (Nouraliee and Ebrahimi, 2012). Based on the geothermometery studies, the Mahallat geothermal reservoir approximate temperature was estimated to vary from 88 to 194 °C (Nouraliee and Ebrahimi, 2012).

Rezaei et al. (2009) presented a conceptual model of hot springs formation in the targeted area. According to their model, rainfalls infiltrate into the earth along the transverse faults, fractures and permeable rocks. The infiltrated waters become more soluble when mixed with vapors and other volatiles (i.e., H_2O and CO_2) due to high pressure. Such materials mainly originated from magma bodies or other high-temperature rocks in the earth. The density of infiltrated waters was subsequently reduced by the increase in their temperature. Such a phenomenon occurs in the depth and in the proximity of cooling magma and/or hot rocks. Moreover, capturing volatile materials can reinforce this process. As a consequence, infiltrated waters become more buoyant and rise up along the faults. During rising and reacting with surrounding carbonate rocks, their temperature decreases, and more volatiles dissolve in the waters. So, the solubility of the hot waters increases, and therefore, deep karst networks are formed in hosting carbonate sequences. Likewise, mixing of hot waters with shallow cool waters can control the dissolution in carbonate intervals. Rising of waters to upper (shallower) levels causes depletion in hydrostatic pressure. All of these have resulted in outgassing (e.g., CO_2) and formation of super-saturated waters with respect to the carbonate calcium ($CaCO_3$). Subsequent precipitation of dissolved carbonate calcium leads to the formation of travertine that we can see around the hot springs.

GRAVITY SURVEY

Data acquisition and reductions

Gravity survey was carried out in Mahallat geothermal field by the Renewable Energy Organization of Iran (SUNA) in 2012. The measurements were made with the Scintrex CG5 gravimeter at 380 stations on an

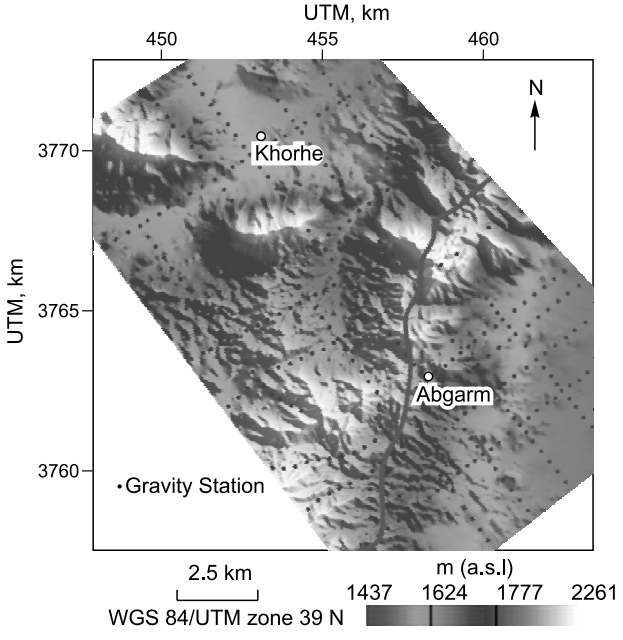

Fig. 2. The topographic map of the study area. The black dots represent the gravity stations.

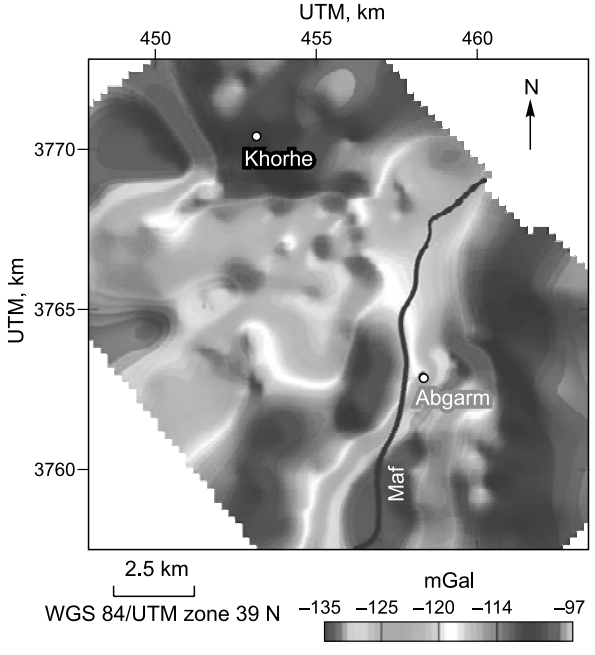

Fig. 3. The complete Bouguer anomaly map of the study area.

area of approximately 200 km^2. Figure 2 shows distribution of the gravity stations in the region. The spacing between the stations varies from 200 m to 450 m, depending on the accessibility of the terrain. Mahallat gravimetric base station (National Cartographic Center of Iran—NCC) was used to correct relative values to absolute gravity. The 3D station coordinates were obtained using trigonometric calculus from topographic survey observations (planimetry and altimetry) performed from geodetic marks. The accuracy of these determinations is about 0.03 m. International Association of Geodesy 1967 formula and the average crustal density of 2.67 g/cm^3 were used for calculating free air and Bouguer corrections. Topographic corrections were reduced using the "Hammer" method over the 1:25,000 topographic maps.

Figure 3 shows the complete Bouguer anomaly map of the study area. In the northern portion of the map (northeast of Khorhe village), there is a high-value anomaly (–110 to –102 mGal) coinciding with the high-density igneous rocks. Also, in the eastern portion of the map (from UTM (X) coordinates ~ 461000 m), there is a prominent high-value anomaly coinciding with the location of travertine and young traces. However, these rocks are characterized by low density and cannot be associated with this gravity anomaly, thus it seems that there is an igneous intrusive body in the subsurface of the locality (Mirzaei et al., 2013). From the south towards Abgarm village, along the MAf zone, there is a low-value anomaly (–129 to –134 mGal), probably related to the fractured zone in the subsurface, as its lithological boundary clearly follows the strong gravity gradient. In addition, there is another prominent negative anomaly east of Khorhe. These negative anomaly areas are considered as probable reservoirs of the geothermal system in the region.

REGIONAL / RESIDUAL SEPARATION

The complete Bouguer anomaly contains superposition of regional and residual anomalies. The regional Bouguer gravity anomaly is resulting from the presence of deeper and broader structures. The residual Bouguer gravity anomaly is resulting from the presence of smaller and more superficial ones. In this work, to highlight the gravity anomalies related to the interesting source, a regional-residual separation of the complete Bouguer anomaly was performed. Correct estimation and removal of the regional anomaly from the observed field yields the residual anomaly produced by the target sources. There are at least four approaches to doing so (Li and Oldenburg, 1998a), from more empirical to the graphical ones (see, e.g., Telford et al., 1990). In the current study, there is a regional trend from the east and the north of the area towards the west. Thus the regional field is estimated by least-squares fitting a second-order polynomial to the observed gravity field, so that this regional trend would not absorb the local gravity anomalies. When the regional field was calculated, it was subtracted from the complete Bouguer field to calculate the residual field. Figure 4 shows the calculated regional and residual fields.

Due to the existence of significant fractures and faults in a geothermal reservoir, low density zones were formed. Therefore, in a geothermal exploration program, generally but not in all cases, negative gravity anomalies are likely places associated with the geothermal reservoir. In the current study area, three negative gravity anomalies (A1, A2, and A3 in Fig. 4) are found in the residual gravity map. Two of them (A1 and A2) are situated along the MAf zone of the area. They constitute a particular interest, as they are related to the main fault where hydrothermal systems are known to exist. A1 anomaly is the most intense negative anomaly in the area and reflects the lower density sedimentary deposits where they are fractured by the main fault. A1 covers a broader area of the survey and consists of many thermal surface manifestations such as hot springs, various alterations and thick travertine layers (Oskooi et al., accepted for publication). This particular site has been subjected to several geophysical surveys, namely magnetic and magnetotelluric (e.g., Oskooi and Darijani, 2013; Oskooi et al, 2013, 2014), thus it is a matter for this study.

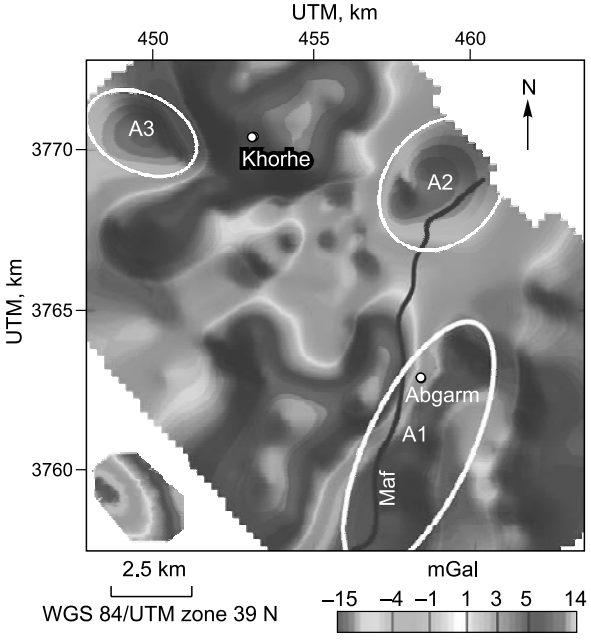

Fig. 4. The residual gravity anomaly map of the study area after separation of the second-order polynomial fitting from the complete Bouguer anomaly. The calculated regional gravity map is depicted on the bottom left corner. A1, A2, and A3 indicate the negative gravity anomalies analyzed in the text.

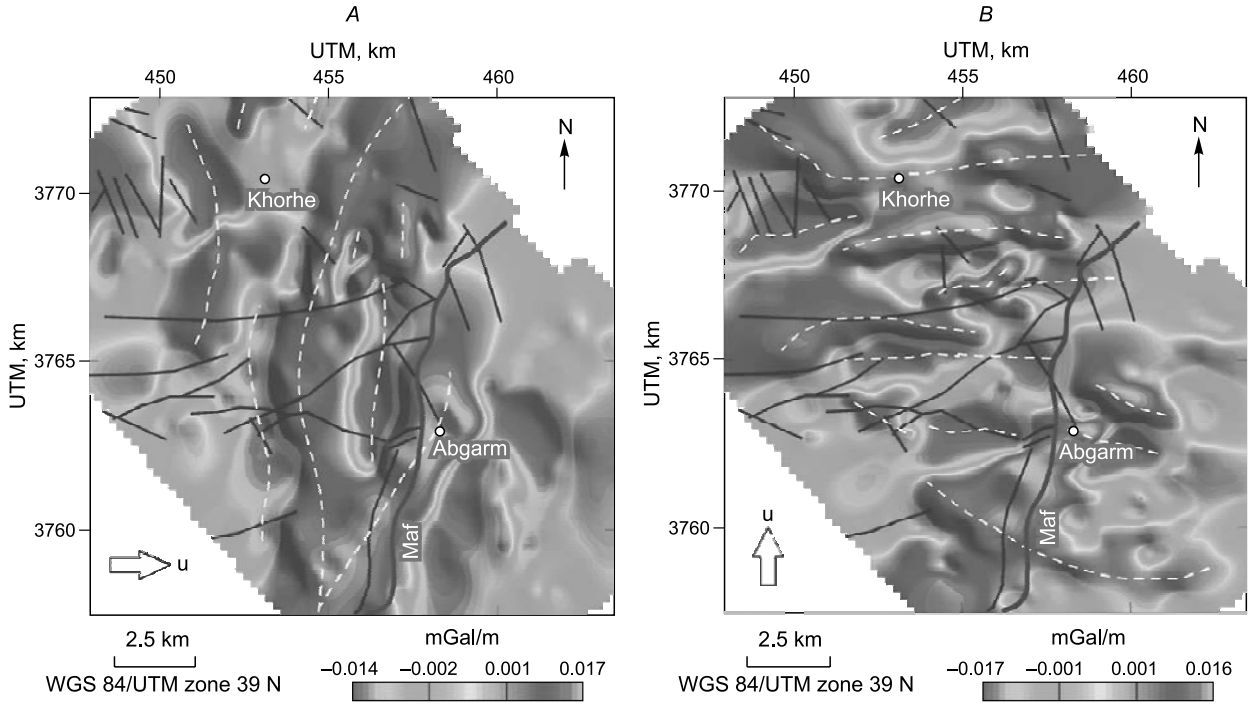

Fig. 5. Directional horizontal gradients of the Bouguer anomaly field along the directions EW (A) and NS (B). The black lines are known faults in geological map and the white dashed lines are discontinuities, identified using the horizontal gradient map.

A2 anomaly is located along the MAf zone of the area and creates a less intense gravity anomaly. A2 seems to be a fractured zone due to MAf zone and can be a candidate for a geothermal reservoir in the area but there are no significant geothermal surface manifestations in this zone. The previous studies (Oskooi et al., 2013 and accepted for publication) and the geological information show that this zone is not fed well by the surface fluids.

A3 anomaly is located in western Khorhe, where there are significant geothermal manifestations. A small and less intense gravity anomaly was detected in A3 zone. It is believed that this anomaly is related to the limestone and sandstone rocks, as a good correlation can be observed between the shape of gravity anomaly and the outcrop of these rocks.

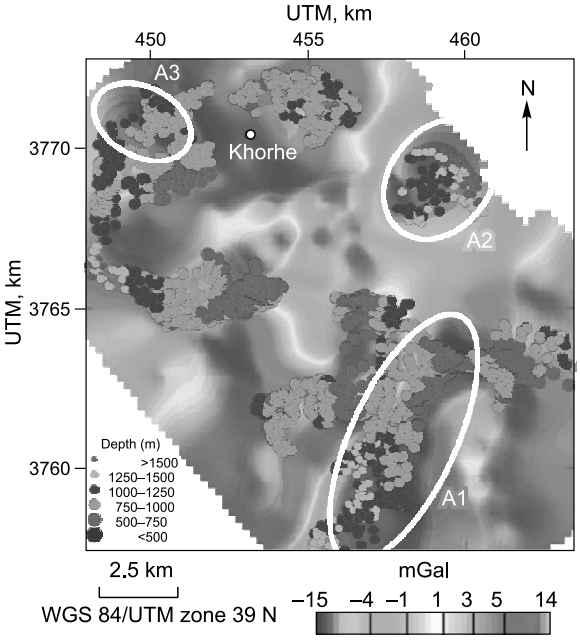

Fig. 6. Euler depth estimation solutions on the residual gravity map.

DIRECTIONAL HORIZONTAL GRADIENTS

Geothermal fields in many sedimentary basins are distributed along the fault-controlled linear trends, and faults detection is often used effectively for target-area selection in geothermal exploration. Also, almost all of geothermal reservoirs in various geologic settings are commonly associated with the fluid conducting faults. In this section, application of gravitational gradients of the study area is reviewed. It shows that directional horizontal gradients are well-suited for investigation of structures, delineation of the faults and their orientations. The first-order horizontal gradient of the gravitational field in a given direction emphasizes the short wavelength spatial components of gravity anomalies and attenuates the long wave-

length spatial components associated with regional trends and large scale anomalies along that direction. This filter enhances the anomalies arising from near source over those arising from deeper or more distant sources. The gradient will reach a minimum/maximum in regions where the density contrast is higher, thus highlighting discontinuities perpendicular to the direction of gradient and detecting more clearly the margins of the structures (Nabighian, 1984).

We used the GRIDGRAD Geosoft extension (available in the Geosoft Oasis Montaj 7.0.1 software) to calculate the horizontal gradient in a specified direction. A 3×3 point convolution filter was applied to the gridded data to produce the gradient results. It is notable that the gradient data contain an inherent zero reference and should not be reduced to residual anomaly data. Therefore in the current study, we used the Bouguer anomaly field for applying the horizontal gradient filter.

The direction of the main fault (MAf) in the study area is approximately N-S. Therefore, two maps of the first-order horizontal gradients were calculated, one along the direction E-W, perpendicular to the direction of the main fault to enhance the structures almost parallel to the main fault (Fig. 6A), and another along the direction N-S, to reveal the structures almost perpendicular to the main fault (Fig. 6B). In Fig. 6, the black lines represent the known faults in the geological map and the white dashed lines are discontinuities, identified using the horizontal gradient map. These maps clearly show the importance of the main lineament, the MAf zone that controls the evolution of the sedimentary basins.

In the central part of the map, in Fig. 6A, the gradients are stronger and the main fault is recognized as strong gradient with a NNE–SSW orientation. In the west of this confirmed main fault, there seems to be another main fault, located almost along that. This lineament doesn't seem to be reflected at the surface faults but the high values of the anomalies suggest that they could have expression in depth and they may represent important discontinuities in lithology. Also, in the map in Fig. 6B, more than 10 main faults (white dashed lines) have been detected using the first-order horizontal gradient. In Figure 6, both proved faults by the geological map (black solid lines) and the faults identified by the horizontal gradients show the mechanism of the complex faults in the Mahallat geothermal field. These faults play an important role in hydrothermal circulations which are acting as preferential paths for the hydrothermal fluids circulating in the area.

EULER DEPTH ESTIMATION

In order to estimate the location of the gravity anomaly sources, we applied the standard method of Euler deconvolution to the data. The Euler method uses three orthogonal gradients of the gravitational field quantity. A 3D form of Euler's equation can be defined (Reid et al., 1990) as,

$$x\frac{\partial g}{\partial x} + y\frac{\partial g}{\partial y} + z\frac{\partial g}{\partial z} + NT = x_0\frac{\partial g}{\partial x} + y_0\frac{\partial g}{\partial y} + z_0\frac{\partial g}{\partial z} + NB \tag{1}$$

where $\partial g/\partial x$, $\partial g/\partial y$ and $\partial g/\partial z$ are the derivatives of the total field versus x, y and z axes, respectively. x_0, y_0 and z_0 are the coordinates of a gravitational source, N indicates the structural index (SI) and relates with the rate of change of a potential field with the distance, and B is the local background representing the "regional" field within a sliding window with adjustable size.

Eq. (1) can be solved in a window centered on a given grid point to find the unknown source point (x_0, y_0, z_0) and the regional field (Reid et al., 1990). This approach introduces a nonlinear relationship between the SI and the unknown regional field. By specifying the SI, Euler's equation is solved using the linear least-squares method (Reid et al., 1990).

Thompson (1982) revealed different values of structural index for the geological geometry. The structural index depends on the source geometry and its range is between 0 to 2 for the gravity sources (and 0 to 3 for the magnetic sources). Stavrev and Reid (2007) show that the structural index depends on the type and physical parameters of the potential field and provides an excellent overview of the parameters of Euler's homogeneity equation in general and the structural index in particular. It is notable that a zero index which implies the potential field is constant, regardless of the distance from the anomaly source. These solutions are physically impossible for real data, and a zero index indicates a physical limit which can only be approached as the so-called "infinite" dimensions of the real source increase. In this case, in practice, an index of 0.5 can often be used to obtain reliable results when an index of zero would indicate otherwise.

In order to obtain reliable results in Euler method, the structural index and the window size must be carefully selected. The window size determines the area in grid cells used to apply Euler deconvolution. All the points within the window are used to solve Euler's equation to locate the source. It should be large enough to incorporate the entire anomaly to be interpreted and small enough to avoid significant effects from adjacent or multiple sources (Bournas et al., 2003). In case of anomalies caused by close sources considered, included in a given window, the uncertainty of the solution will increase.

In order to apply Euler method to gravity data of Mahallat region, we used the package of Geosoft Oasis Montaj® software. After preparing of data grid, we applied gravitational field derivatives in three directions of *x, y*, and *z* which are necessary for the Euler deconvolution process. Then, structural index and window sizes were selected appropriately. To attain the most reliable structural index, different values were tested. Since we had no idea about the geometry of the gravity anomaly source, we tested structural indices from 0.5 (for dyke) to 2 (for sphere) by steps of 0.1. Finally, an appropriate structural index was estimated to be between 1.2 and 1.4. Structural indices in this range suggested the best clustering and regularity in the solutions. Therefore, we considered a value of 1.3 for structural index as an average. Then Euler method was applied to residual data by moving different window sizes. The best results were attained by a window size of 200 m × 200 m, while the structural index was fixed to be equal to 1.3.

Figure 6 shows Euler depth estimation solutions on the residual gravity map using the structural index of 1.3. In this figure, Euler solutions on the residual gravity map show different depths for different anomalies. The estimated depth for both positive and negative anomaly sources in the current area lies in the range between 500 m and 2000 m. The depth values estimated in the negative zones (A1, A2, and A3 in Fig. 6) range from about 500 m to 2000 m. Based on the Euler depth estimation, estimated depth for the negative anomaly source in zone A1 starts from about 500 m in the northern part of this zone, while it is located at about 1500 m in the southern part of zone A1 along the MAf zone. Also, in zone A2, estimated depths of the negative anomaly sources range from about 1000 m to 2000 m and for zone A3 from 750 m to 1000 m. The estimated depths in these zones can be interpreted as the depth of the geothermal reservoirs in the Mahallat geothermal region.

3D INVERSION

The three-dimensional density contrast model was calculated with the UBC-GIF Grav3D software with the algorithms of Li and Oldenburg (1998), which often provided interesting results (e.g., Oldenburg and Pratt, 2007; Kalate and Kahoo, 2013; Louro and Mantovani, 2013). This algorithm starts from Eq. 2:

$$d = G\rho \tag{2}$$

where d is the vector of real extracted in the survey, G is the sensitivity matrix and ρ is the density vectors of the tri-orthogonal mesh to be created for the inversion.

The inverse problem can be formulated as an optimization problem where an objective function of the model is minimized, subject to the constraints in Eq. 2. The objective function of the density model in Eq. 3 is minimized under determined constraints in order to reproduce the data inside an error tolerance.

$$\phi_m = \alpha_S \int_v w_s w^2(z)(\rho-\rho_0)^2 dv + \alpha_x \int_v w_x \left\{\left[\frac{\partial w(z)}{\partial x}\right](\rho-\rho_0)\right\}^2 dv +$$

$$+\alpha_y \int_v w_y \left\{\left[\partial w(z)/\partial x\right](\rho-\rho_0)\right\}^2 dv + \alpha_z \int_v w_z \left\{\left[\partial w(z)/\partial x\right](\rho-\rho_0)\right\}^2 dv \tag{3}$$

where m is gravimetric model element, ρ_0 the reference model, w_S, w_x, w_y, and w_z weighting functions, α_S, α_x, α_y, and α_z coefficients which affect the relative importance of different components in the objective function and $w(z)$ a generalized depth weighting function. This function has flexibility in constructing a variety of models. The aim of the objective function is to counteract the geometrical decay of the sensitivity with the distance from the observation location, so that the recovered density is not concentrated near the observation locations. In the next step, the data misfit (ϕ_d) between the observed data and the predicted data is calculated, using Eq. 4:

$$\phi_d = \|w_d(d_{\text{mod}} - d_{\text{obs}}\| \tag{4}$$

Table 1. **Average densities for the main rock types in the study area (After Telford et al., 1990)**

Rock type	Average density (kg/m^3)
Limestone	2700
Dolomite	2550
Sandstone	2350
Shale	2530
Granite	2690
Granodiorite	2730

w_d is a diagonal matrix in which the ith element is the standard deviation of the ith datum, d_{mod} the predicted density and d_{obs} the observed data. The inversion objective is to minimize the difference between both the objective function and the data misfit:

$$\phi = \phi_d + \mu\phi_m \tag{5}$$

In which μ is a regularization parameter that controls the relative importance of the model norm and the data misfit.

The described methodology provides a basic structure for solving 3D gravimetric inversion. More solutions of Grav3D are available in Li and Oldenburg (1998).

In this approach, the 3D subsurface volume of the ground is discretized using a mesh file, the parameters of which are defined by the user. The mesh should be designed in accordance with the vastness of the area and the desired resolution. The size of the cells within the mesh determines the resolution of the model. The cell size depends on the scale of the study area and the mean distance between the gravity measurements. In the current inversion, a cell size of 100 meters was set for the mesh, which was considered an appropriate compromise between the model discrimination and the model resolution.

The inversion method requires specifying the upper (maximum) and lower (minimum) bounding values for density contrast of each cell at the beginning of the process. Table 1 shows the main rock densities, which constitute the structure of the Mahallat geothermal system. In the current study area, based on the rock density table, the upper and lower bounding values of density contrast were set to -500 kg/m^3 and 500 kg/m^3, respectively. Also, other density ranges were tested, but the above-mentioned selected range was the one that provided a model which showed the best agreement with the available geological data.

Inversion of the residual gravity data using Grav3D software (Li and Oldenburg, 1998) resulted in a density contrast which is shown in Figs. 8 and 9. In these Figures, the high density rocks are marked with the dark color and the low density rocks are shown with the light color.

Figure 7 shows the slices of the density contrast model at five different depths (500, 1000, 2000, 3000, and 4000 m). At about 500 m depth (Fig. 7), calculated model shows several small anomalies. In zones of A1 and A3, these anomalies are very significant but in zone A2 they are not clear. At the depth of about 1000 m (Fig. 7), in zones A1 and A2, more distinct negative density contrasts were created, and these contrasts also can be seen at the depth of more than 2000 m. From the depth of around 3000 m and more, the density contrasts have been smoother, as shown in Fig. 7.

Sedimentary rocks are usually less dense than igneous and metamorphic rocks (see Table 1). A wide range of density of sedimentary rocks is observed, which is primarily due to variation in porosity (Telford et al. 1990). The nature of the pore fluids also affects the bulk density. All types of rocks, especially the sedimentary ones, are influenced by age, previous history and depth of burial. In general, although some previous histories of rocks increase density, such as compaction by depth and time, some other ones decrease the density of rocks, such as pores and faults. Under normal conditions, the density contrast between adjacent sedimentary formations in the field is seldom greater than 250 kg/m^3, except for a fractured zone.

In the current study, the MAf has produced a fractured zone in limestone rocks (possible reservoir rock in the study area). According to geological and hydrochemical studies, it is considered that carbonate rocks host the geothermal reservoir of Mahallat region. These rocks are formed of limestone (with density of 2700 kg/m^3) surrounded by mostly dolomites (with density of 2550 kg/m^3). Therefore, the density contrast of less than –150 kg/m^3 can be considered for reconstruction of the reservoir model during 3D inversion. In other words, based on the table of rock densities, we considered the areas with density contrast of less than –150 kg/m^3 as suitable places for containing of geothermal reservoirs in the study area. In Fig. 8, the recovered model is depicted in a perspective view at cutoff lower than –150 kg/m^3. Regarding this figure, the main fault of the area is responsible for a negative density contrast of rocks. As expected, based on the gravitational field maps, zone A1, which corresponds to this fault, shows an area of considerable negative density contrast at all of the depths. This area has a more continuous extension to the depths of 1000 to 3000 m, which suits the

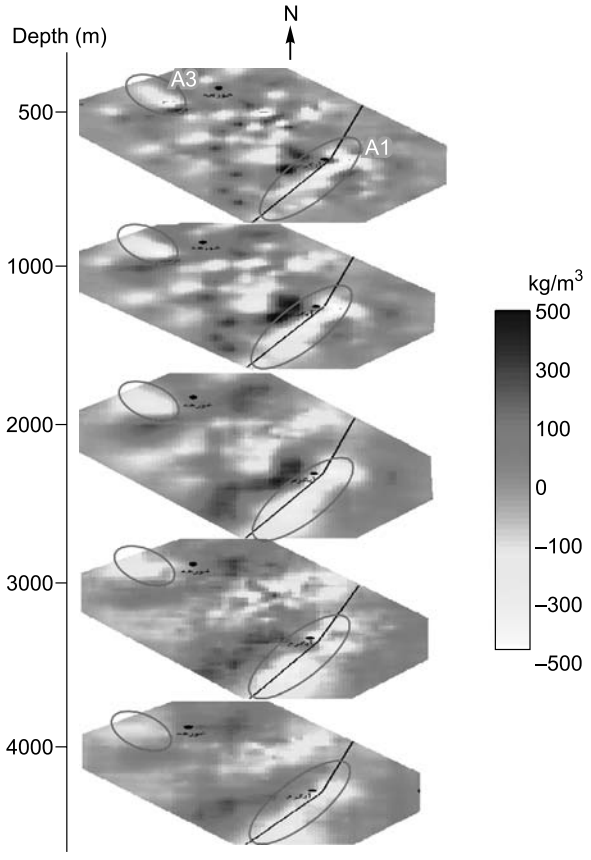

Fig. 7. First 4000 m of the 3D density contrast model in the Mahallat geothermal field calculated using the Li–Oldenburg (1998) method.

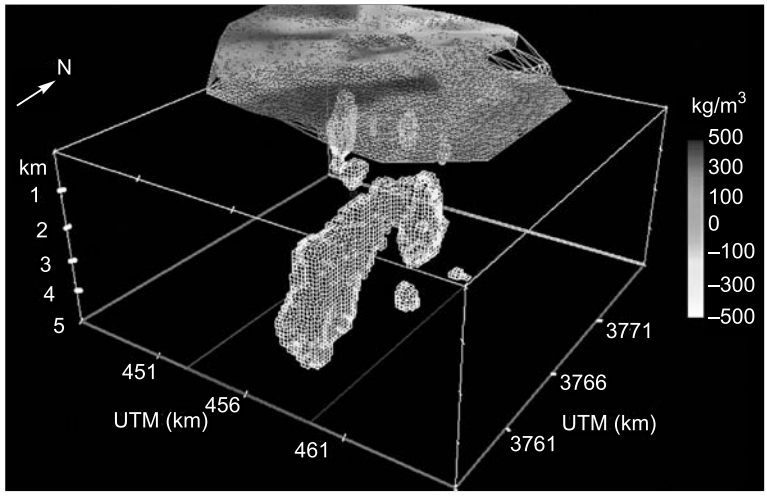

Fig. 8. The 3D model of the contrast density lower than 150 kg/m^3 of the first 5000 m in the Mahallat geothermal field using the Li–Oldenburg (1998) method.

anomaly. Thus, it seems that the geothermal reservoir has higher quality at this depth. The activity of MAf zone, together with its tributaries, has resulted in the formation of many fractures and joints in the rocks. As a result, an appropriate space for circulation of hydrothermal fluids was prepared in the rocks of zone A1 at depths between 1000 and 3000 m, so indicating of an important geothermal reservoir in this zone. These results are supported by geothermal surface manifestations in this area (A1 zone), such as hot springs and intense hydrothermally altered areas.

The other lesser noticeable area of negative density anomaly is zone A3, located in the western part of Khorhe village. This zone is as small as zone A1 (Figs. 7 and 8). Although, the best place for formation of geothermal reservoir in this zone is at the depth between 1000 and 2000 m, where the negative density contrast is considerable (see Figs. 7 and 8), the lack of significant geothermal surface manifestations found in this zone indicates that this zone cannot be a suitable candidate for a possible geothermal reservoir in the region or maybe it is a hidden or blind geothermal system. No doubts, more scientific data would be needed to prove this theory.

CONCLUSION

Mahallat geothermal region is one of the most interesting localities for geothermal exploration in Iran. This paper presents the interpretation of the gravity data over this area, around the Mahallat–Abgarm fault (MAf). Analysis of the residual gravity field shows three negative anomaly zones (A1, A2, and A3) which can be associated with the geothermal reservoirs in the area. The results of the horizontal gradient filters show the most of the observed anomaly to be associated with faults and geological contacts. The main structure, the MAf zone, has a strong expression in the direction of NNE-SSW, and most of the geothermal surface manifestations in the region exist along this fault. It seems that the most important negative anomaly zone in the residual gravity map (A1) is due to this fault. The 3D inversion of gravity data gives an image of the evolution of the density contrast at different depths. The most significant aspect is the evolution in depth of the negative anomalies in A1 and A3 zones. The 3D recovered model shows a large negative density contrast at the depths between 1000 m and around 3000 m in A1 zone, which can result from high fractured rocks and the activity of the main fault, allowing for comfortable hydrothermal fluid circulation consequently. At the same point, A3 zone is partly considerable to allow a negative density contrast and as consequence is suitable for a geothermal reservoir. The results of the Euler depth estimation, the 3D inversion and the geothermal surface manifestations in A1 zone, such as hot springs and intense hydrothermally altered rocks, and lack of these manifestations in A3 zone indicate high potential for geothermal reservoir forming in A1 zone along the main fault, at the depths between 1000 m and around 3000 m. Also, the results of the Euler depth estimation and the 3D recovered model of density contrast show the thickness of this identified geothermal reservoir to increase from Abgarm village toward SSW along the main faults.

This work also revealed the importance of the gravity survey and its data interpretation to ensure better understanding of the relationship between the geothermal reservoirs and the negative density contrasts.

ACKNOWLEDGMENTS

The authors wish to thank the Renewable Energy Initiative Council of Vice-Presidency of Scientific and Technology and Niroo Research Institute (NRI) for providing gravity data for this study. The authors would also like to thank Hamzeh Mehrabi and Amir Hossein Enayati for their useful geological comments.

REFERENCES

Abiye T.A., Haile T. Geophysical exploration of the Boku geothermal area, Central Ethiopian Rift // Geothermics, 2008, v. 37 (6), p. 586–596.

Beitollahi A. Travertine formation and the origin of the high natural radioactivity in the region of Mahallat hot springs. The M.Sc. Thesis. Islamic Azad University of Tehran, Iran, 1996, 120 pp.

Bournas N., Galdeano A., Hamoudi M., Baker H. Interpretation of the aeromagnetic map of Eastern Hoggar (Algeria) using the Euler deconvolution, analytic signal and local wavenumber methods // J. Afr. Earth Sci., 2003, v. 37 (3), p. 191–205. DOI: http://dx.doi.org/10.1016/j.jafrearsci.2002.12.001.

Giggenbach, W.F. Chemical techniques in geothermal exploration // D'Amore, F. (coordinator), Applications of geochemistry in geothermal reservoir development. UNITAR/UNDP publication, Rome, 2008, p. 119–142.

Gottsmann, J., Camacho, A.G., Martí, J.,Wooller, L., Fernández, J., García, A., Rymer, H. Shallow structure beneath the Central Volcanic Complex of Tenerife from new gravity data: implications for its evolution and recent reactivation // Physics of the Earth and Planetary Interiors, 2008, v. 168, p. 212–230.

Kalateh A.N, Kahoo, A.R. Estimation of 3D density distribution of chromite deposits using gravity data. J. Mining Environ., 2013 v., 4, p. 97–104.

Li, Y., Oldenburg, D.W. Separation of regional and residual magnetic field data // Geophysics, 1998a, v. 63, p. 431–439.

Li, Y., Oldenburg, D.W. 3D inversion of gravity data // Geophysics, 1998b, v. 63, p. 109–119.

Louro, V.H.A., Mantovani, M.S.M. 3D inversion and modeling of magnetic and gravimetric data characterizing the geophysical anomaly source in Pratinha I in the southeast of Brazil // J. Appl. Geophys., 2012, v. 80, p. 110–120.

McKenzie D.S. Active tectonics of the Mediterranean region. Geophys. J. R. Astron. Soc., 1972, v. 30, p. 109–185.

Mirzaei, M., Moghaddam, M.M., Oskooi, B., Ghadimi, F., Jazayeri, S. Processing and interpretation of ground magnetic data corresponding to geothermal resources using Euler and AN-EUL method, north-east of Mahallat // J. Earth Space Phys., 2013, v. 39, p. 83–96.

Montesinos, F.G., Camacho, A.G., Nunes, J.C., Oliveira, C.S., Vieira, R. A 3-D gravity model for a volcanic crater in Terceira Island (Azores) // Geophys. J. Int., 2003, v. 154, p. 393–406.

Nabighian, M.N. Toward a three-dimensional automatic interpretation of potential field data via generalized Hilbert transforms: fundamental relations // Geophysics, 1984, v. 49, p. 780–786.

Nouraliee, J., Ebrahimi, D. Geochemical studies in Mahallt geothermal region, internal report [in Persian]. Niroo Research Institute (NRI), Tehran, Iran, 2012.

Nouraliee, J., Shahhosseini, A. Geological map of Mahallat geothermal region, Scale: 1:25,000. Niroo Research Institute (NRI), Tehran, Iran, 2012.

Oldenburg, D.W., Pratt D.A. Geophysical inversion for mineral exploration — A decade of progress in theory and practice // Ed. B. Milkereit, Proceedings of Exploration 07: Fifth Decennial International Conference on Mineral Exploration, 2007, p. 61–95.

Oskooi, B., Darijani, M. 2D inversion of magnetotelluric data from Mahallat geothermal field in Iran using finite element approach // Arabian J. Geosci., 2013, doi:10.1007/s12517-013-893-6.

Oskooi, B., Darijani, M., Mirzaie, M. Investigation of electrical resistivity and geological structure on the hot springs in Markazi province of Iran using magnetotelluric method // Bollettino di Geofisica ed Applicata, 2013, v. 54, p. 245–256.

Oskooi, B., Mirzaei, M., Mohammadi, B., Moghaddam, M.M., Ghadimi, F. Integrated interpretation of the magnetotelluric and magnetic data from Mahallat geothermal area, Iran // Studia Geophysica et Geodaetica (accepted for publication).

Pentecost A. Travertine. Berlin, Springer-Verlag, 2005, 449 pp.

Porkhial, S., Nouraliee, J. Rahmani, M., Ebrahimi D. Resource assessment of Vartun geothermal region, central Iran // J. Tethys, 2013, v. 1, p. 29–40.

Reid A. B., Allsop J.M., Granser H., Millet A.J., Somerton, I.W. Magnetic interpretation in three dimensions using Euler deconvolution // Geophysics, 1990, v. 55, p. 80–91.

Represas, P., Santos, F.A., Ribeiro, J. Interpretation of gravity data to delineate structural features connected to low-temperature geothermal resources at Northeastern Portugal // J. Appl. Geophys., 2013, v. 92, p. 30–38.

Rezaie M., Ghorbani M., Bomeri M. The hydrogeology and geothermology of the Mahallat hot springs // 1st National Conference on Hydrogeology, Behbehan, Iran, Extended Abstract, 2009, 4 pp.

Salem, A., Furuya, S., Aboud, E., Elawadi, E., Jotaki, H., Ushijima, K. Subsurface structural mapping using gravity data of Hohi geothermal area, Central Kyushu, Japan // Proceedings of World Geothermal Congress, Antalya, Turkey, 2005.

Schiavone, D., Loddo, M. 3-D density model of Mt. Etna Volcano (Southern Italy) // J. Volcanol. Geotherm. Res., 2007, v. 164, p. 161–175.

Soengkono, S. Deep interpretation of gravity and airborne magnetic data over the Central Taupo Volcanic Zone // New Zealand Geothermal Workshop, 2011.

Soligo, M., Tuccimei, P., Barberi, R., Delitala, M.C., Miccadei, E., Taddeuci, A. U/Th dating of freshwater travertine from Middle Velino Valley (Central Italy): paleoclimatic and geological implications // Palaeogeogr. Palaeoclim. Palaeoecol., 2002, v. 184, p. 147–161.

Stavrev P., Reid A. Degrees of homogeneity of potential fields and structural indices of Euler deconvolution // Geophysics, 2007, v. 72 (1), L1–L12, DOI: 10.1190/1.2400010.

Telford, W.M., Geldart, L.P., Sheriff, R.E. Applied geophysics, 2nd edition. Cambridge University Press, 1990.

Thompson D.T. EULDPH a new technique for making computer-assisted depth estimates from magnetic data // Geophysics., 1982, v. 47, p. 31–37.

Рекомендована к печати 28 мая 2015 г.
А.Д. Дучковым

Поступила в редакцию
26 декабря 2014 г.